EXPERIMENTAL AND NUMERICAL STUDY ON THE MITIGATION CAPABILITY OF SOME SPECIAL DESIGN STRUCTURES

Florina Bucur, Adrian Rotariu, Eugen Trană, Amado Ștefan

"Ferdinand I" Military Technical Academy, Bucharest, Romania

Corresponding author: Eugen Trană, eugen.trana@mta.ro

Abstract: The ballistic protection for military personnel and military vehicles represents an important aspect in the design of future generations of military vehicles. In the current paper an experimental and numerical study regarding blast wave mitigation capacity of two special design structures is performed. The two designs refer to a V-shape structure and a bilayer one with an expanded perlite layer placed in front of a steel plate. The impulse mitigation based on the level of steel plate plastic strain and stress is assessed for each tested design. The tests were performed based on the scaling procedure and NATO standards.

Key words: design, blast load, stand-off distance, impulse, mitigation

1. INTRODUCTION

Many of the military vehicles of the last century are based on a simple design concept that implies a simple armor steel as a plane floor and a ground clearance that do not exceed 500 mm. Faced to the most complex threats in military operation theaters, mines and IEDs, this solution doesn't have the ability to protect the crew and assure the vehicles integrity. This is why the new design concepts must consider the battlefield realities and came with new and efficient geometries and materials able to withstand the impulsive loads due to attacks involving the use of energetic materials and explosives [1, 2, 3, 4, 9, 10, 12].

As a consequence of the previously - mentioned issues, all over the world new and ingenious structure were proposed and studied. Among these new solutions the V-shape geometry and bilayer floor structure were extensively studied [5, 6, 7, 8].

As a result, nowadays, the most used solutions applied to military vehicles involve greater ground clearance and double floor with a 'V', partially 'V' or curved shape as an exterior floor plate [14, 15, 16].

This solution allows increasing the distance between the crew and the ground and at the same time ensures a movement decoupling between the exterior and interior floor. As a result, the accelerations induced to the inside floor will be greatly diminished compared to the exterior one.

Another advantage of the new design criteria is that heightening the entire vehicle will reduce the impulse by increasing specific Z number [1].

Also, by changing the exterior shape will reduce the floor reflected pressure and the gases action time on the floor (it was proven that a V plate can reduce by 50% the pulse comparatively to a flat plate for the same Z [17]).

But all these advantages are accompanied by a great disadvantage, namely a loss of mobility which is translated in a potential target attitude like. In other words, providing protection measures against land mines will increase vehicle's vulnerability to other threats (amour piercing projectiles, missiles or rocket propelled projectiles).

Considering the already available international studies [4, 18, 19, 22], the scaling law [20] and NATO recommendations [2], the present study was focused on the numerical and experimental investigation of the mitigation ability of a 'V' shape geometry and a bilayer structure (perlite layer placed in front of a steel plate) as a part of an effort to minimize the previously - mentioned disadvantage.

The present experimental and numerical study was performed upon a scaled structure (1:6) according to STANAG 4569 Level 3B [2] requirements for both configurations.

For the numerical study a mixed approach of the Finite Element Method (MEF) [11, 13, 21] with the Smoothed Particle Hydrodynamics Method (SPH) was used. The numerical simulations were performed using AUTODYN® solver.

2. EXPERIMENTAL PART

The proposed test program aimed to estimate the wave shock mitigation ability of three configurations: standard plate, V-shaped plate with 120° peak angle and a bilayer plate – granular material (perlite)-metal plate.

In all configurations a carbon steel (OL50) was used as metallic plate. OL50 has a wide applicability being able to withstand high mechanical loadings due to a

290 MPa yield stress, 490 MPa tensile strength, 240-290 MPa fatigue strength, $20.1 \cdot 10^4$ MPa Young modulus, $8.25 \cdot 10^4$ MPa shear modulus, 160-200 HB hardness and 21% breaking elongation.
For the bilayer configuration, considering the fact that the granular materials are an efficient solution in blast mitigation, for the add-on material, a volcanic rock, namely perlite was chosen. The perlite is a conglomerate of solid and macroscopic particles characterized by a loss of energy when the particles interact. Based on studies available in literature [23, 24, 25] the behavior of perlite corresponds to a plastic-elastic material when is subjected to different types of loads.
As previously stated, the test program was based on the design of a 1:6 scale protection structure able to ensure a NATO Level 3B protection level. The tests considered approx. 11,000 kg structure. The final dimensions resulted from scaling process [5, 20] are shown in Table 1.
The design concepts for vehicle floor are presented in Figure 1.

Table 1. Scaling results

Parameters	Linear scaling					
	Length, mm	Width, mm	Thickness, mm	Ground clearance, mm	Total mass, kg	Explosive charge
Real model	6000	1200	12	850	10,985	8 kg TNT
Scaled model	1000	200	2	141.6	50.852	30 g C4

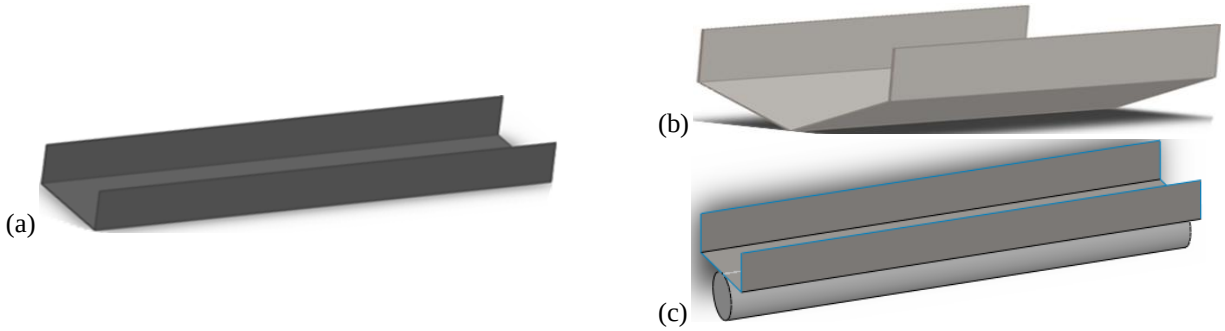

Fig. 1. Testing configurations: (a) standard plate, (b) V-shaped plate with 120° peak angle, (c) bilayer plate (perlite - OL50)

A special concern during experimental tests was paid to make sure that the generated blast wave of the scaling charge corresponds to the blast wave of the real battlefield charge that acts on a full-scale vehicle. For that, based on the STANAG 4569 recommendations, the surrogate explosive charge (C-4 plastic explosive in the form of cylindrical cylinders with a radius of 22.1 mm and a mass of 30 g) was encapsulated in a polystyrene envelope and then fixed in the special container. The special steel-pot made with a cavity for inserting the detonating electric blast cap was placed on the soil surface below the structure center, at the same level as the ground level.
The experimental data were recorded via a high-speed video camera and an acquisition measuring system with accelerometers and pressure transducers.
A schematic of transducer sensors location is depicted in Figure 2: one PCB 102B06 pressure transducer was located on the measuring tool above the center of the test plate, one PCB 350B21 accelerometer on the right side of the support in the central area and one PCB 102B04 pressure transducer was mounted in the proximity of the structure. The location of side-on and face-on pressure transducers was chosen in order to measure both the static and reflected pressure.
For data processing and acquisition a system PicoScope® 6 - PC Oscilloscope was used. The data were recorded and saved in notebooks through the acquisition software, and were later analyzed and processed.
Regarding the ultra-fast shooting camera location, the camera was placed at a 15 meter safety distance from the test site with the lens centered on the test bench. Ultra-fast filming allowed the collection of data on the evolution of the system velocity after the interaction between the shock wave and the studied structure.
For all 3 set-up configurations 2 tests were performed.
The stand-off distances were as follows: 141.6 mm for standard plate, 79 mm for V-shape plate and 41.6 mm for bilayer plate.
Experimental range tests were conducted in a special proving ground.
For reference plate and V-shape plate a 2 mm plate OL50 steel was used.

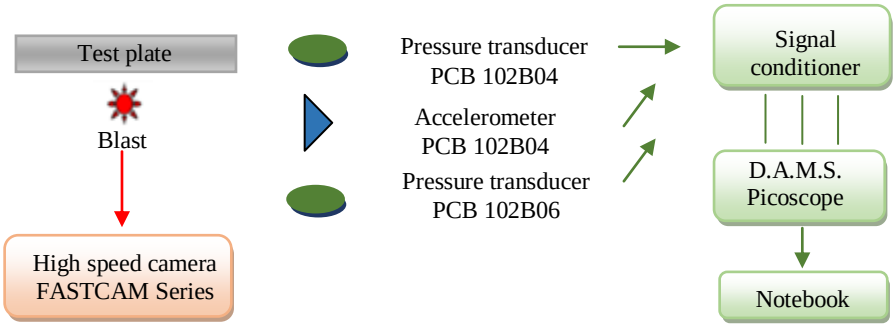

Fig. 2. General configuration of equipment used for experimental research

In Figure 3 is presented the fully equipped test set-up. For the bilayer plate a hermetic bag of plastic foil with a diameter around 100 mm and 1000 mm length was attached to the standard plate facing the blast wave. The bag contained a quantity of 400 g perlite.

In Figure 4 is illustrated the fully equipped test set-up. Post-test activities involved plate deflection measurements. As presented in Figure 5 and Table 3 the response patterns of tested plates subjected to blast wave indicates a dishing failure type for (a) and (c) cases and a loss of plane symetry for case (b), respectively.

Fig. 3. Experimental set-up for OL50 plates

Fig. 4. Experimental set-up for bilayer plate

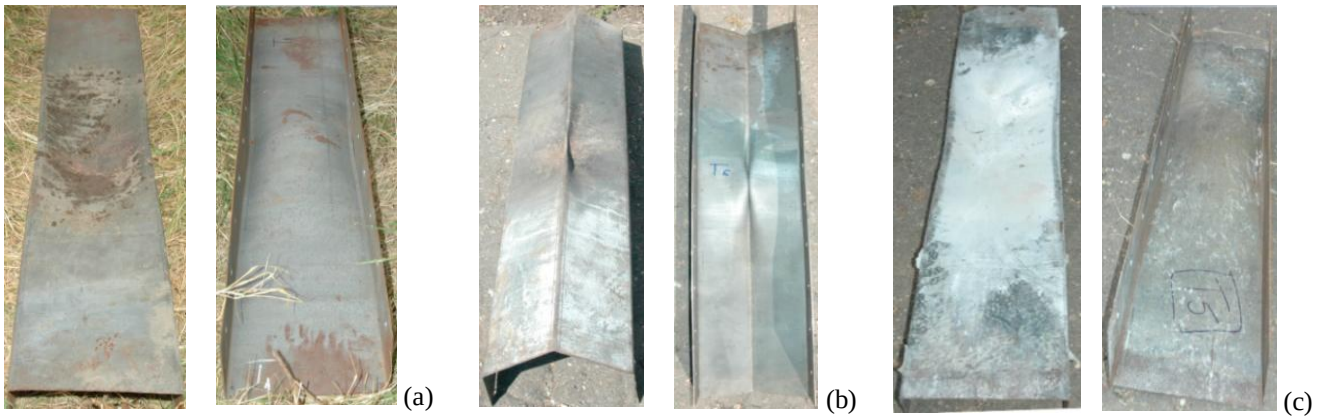

Fig. 5. Blast wave effects upon: (a) standard plate, (b) V-shaped plate, (c) bilayer plate

3. NUMERICAL SIMULATION

The 40ms 3D numerical simulation of experimental tests was performed with the help of AUTODYN® solver. Model set-up is similar to those presented in [5]. The virtual model for the test platform consisted of 25,456 elements of 5 x 5 mm Quad type.

In addition, 16,000 extra elements were used for the flat plate test respectively 17,200 square elements for the V-shaped plate. In order to ensure blast wave interaction with the tested structures a 140 x 400 x 600 mm^3 Euler part was defined and filed with air characterized by a linear EOS.

For the bilayer plate case model, a 100 mm diameter and 0.0079 m^3 volume SPH part (a specific solver implemented in AUTODYN® software) was added

to model the expanded perlite presence.The particles size was imposed to be 5 mm and were wrap-up in a 0.01 mm aluminium thin-film roll. As a result, a number of 59,000 particles were generated. For the thin aluminum film shell elements were considered allowing us to overcome the issue of SPH-EULER solvers non-interaction. This foil had negligible properties and ensured that the total impulse transfers from the shock wave to the structure (as can be see in Table 3).

To measure the blast wave parameters during the test and for a better understanding of the results, AUTODYN® virtual transducers options was used. The positions of the virtual transducers, the plate's geometries as well as the position of the additional material are illustrated in Figure 6.

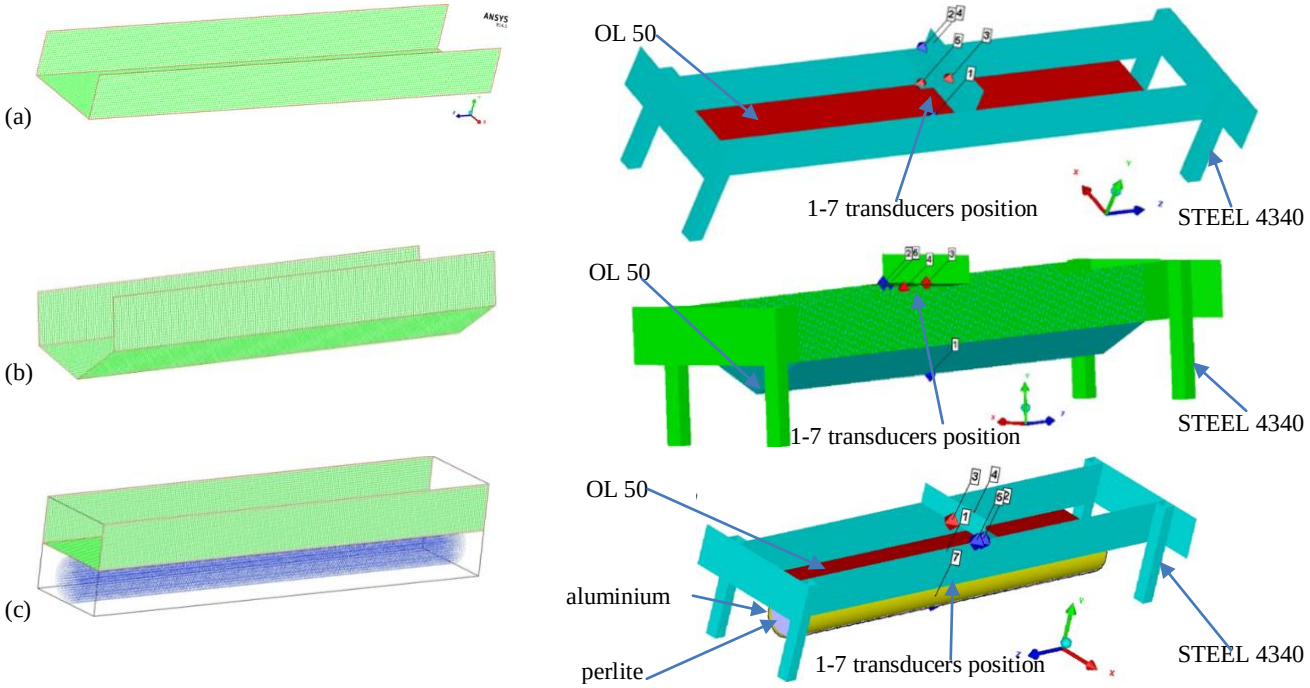

Fig. 6. Test set-up and transducers position: (a) standard plate, (b) V-shape plate, (c) bilayer plate

For some model parts were used materials models already implemented in AUTODYN® Library: STEEL 4340 for test rig, AIR for surroundings environment, C4 for explosive charge and AL5083H114 for aluminum foil.

For the OL50 material a Johnson-Cook constitutive model was imposed. The model parameters are detailed in Table 2. As for the porous granular material, the CRUSHABLE FOAM material model was chosen. The model parameters are also presented in Table 2. The option of crushable foam model was adopted due to the foam like behavior of the perlite as the shock wave passes through.

The OL50 and perlite materials parameters were determined from previously - published data [5, 24].

Regarding the blast wave, a 2D model was initially created and run until the phenomenon does not permit anymore the defining of a symmetry axis, more exactly just before the interaction with the tested structure.

At t = 0.0144 ms, the blast wave was transferred in the 3D models using the REMAP option.

Propagation and interaction of shock wave with the three studied geometry concepts of vehicle floor are illustrated in Figure 7.

The use of the SPH method allows visualization of the granular material dispersion upon shock wave passage, as shown in Figure 8. At t = 0.07 ms the aluminum foil was removed.

For this particular configuration the shock wave initially interacts with the perlite layer which takes some of its energy and transfers to the structure a mitigated impulse. The impulse and energy load the structure in two steps: the first is short and fast and takes place in the first 0.2 ms when an 80% of the impulse is transferred while the second is slow and lasts until the end of the test when accelerated perlite continues to transfer the energy and impulse to the plate.

The effects of the blast wave on test plates in terms of acceleration and overpressure can also be seen from the data recorded by the virtual transducers. The evolution of the signals recorded by the virtual transducers corresponding to the velocity and overpressure parameters is depicted in Figure 9.

Table 2. Material models [5, 24]

Material name	OL 50	Expanded PERLITE			
Reference Density(g/cm^3)	7.81	0.063			
Equation of state	Linear	Linear			
Reference Temperature(K)	293	293			
Bulk Modulus (kPa)	$1.75 \cdot 10^8$				
Strength Materials					
Constitutive Model	Johnson Cook	Crushable Foam			
Shear Modulus (kPa)	$8.08 \cdot 10^7$	1			
Yield Stress (kPa)	$3.42 \cdot 10^5$	Compaction curve			
		10 points			
Hardening constant (kPa)	$3.005 \cdot 10^5$	volumetric strain		compressive stress (kPa)	
Hardening Exponent	0.24	0.089487	0.077761	49.82	310.5
Strain rate constant	0.022	0.18179	0.087419	85.37	465.89
Thermal Softening Exponent	1	0.297059	1.064211	133.3	806.9
Melting Temperature (K)	$1.811 \cdot 10^3$	0.041946	1.324259	183	1971000
Reference Strain Rate	1	0.561242	0.419460	225.5	6035000

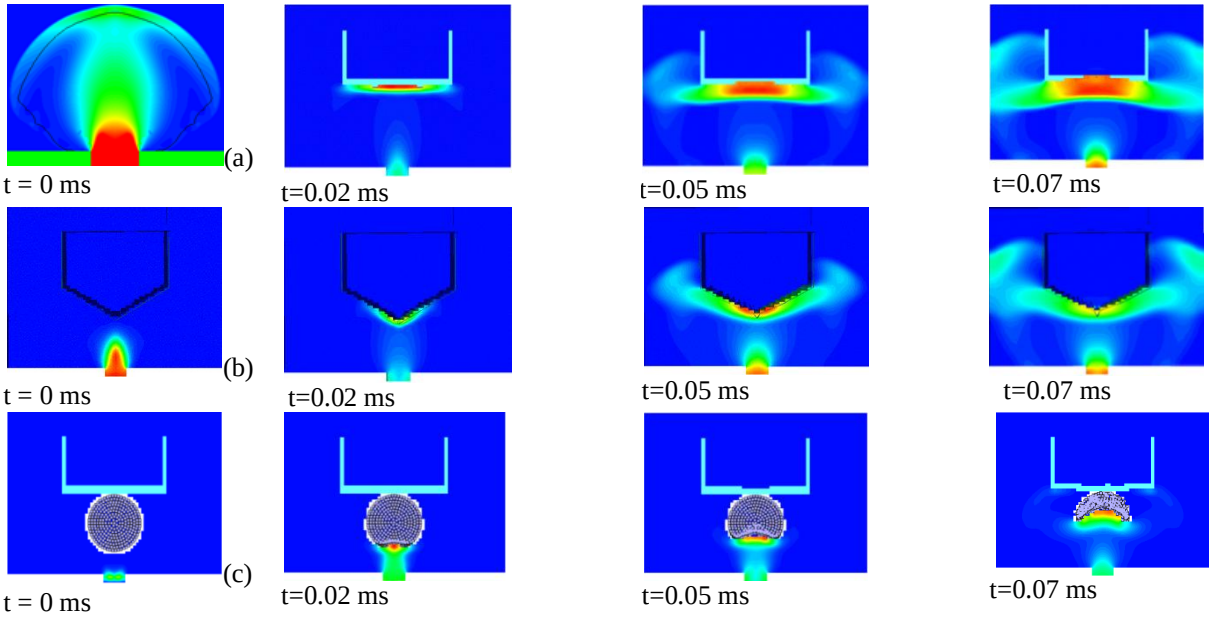

Fig. 7. Formation and blast wave propagation in 3D model: (a) standard plate, (b) V-shape plate, (c) bilayer plate

Fig. 8. Behavior of granular material subjected to blast wave

The AUTODYN® solver interface allows also the extraction of relevant data during the interaction between the shock wave and the analyzed structures regarding the displacements, deformations and stresses.The Iso-values of maximum effective plastic deformations reached in the test plate after t = 40 ms and the Von Mises stress Iso-values fields in plate structure after shock-wave interaction are depicted in Figure 10.

For the same time value, as can be seen in Figure 10, for V-shape plate, the strains are localized especially on the top angle zone.

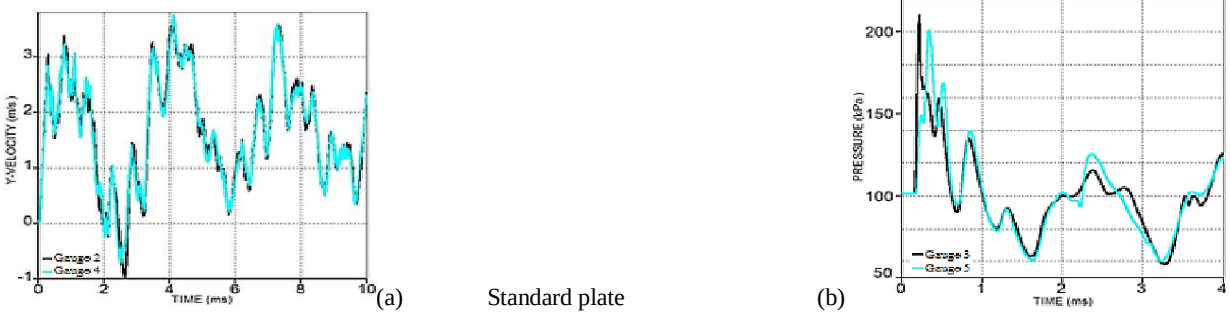

(a) Standard plate (b)

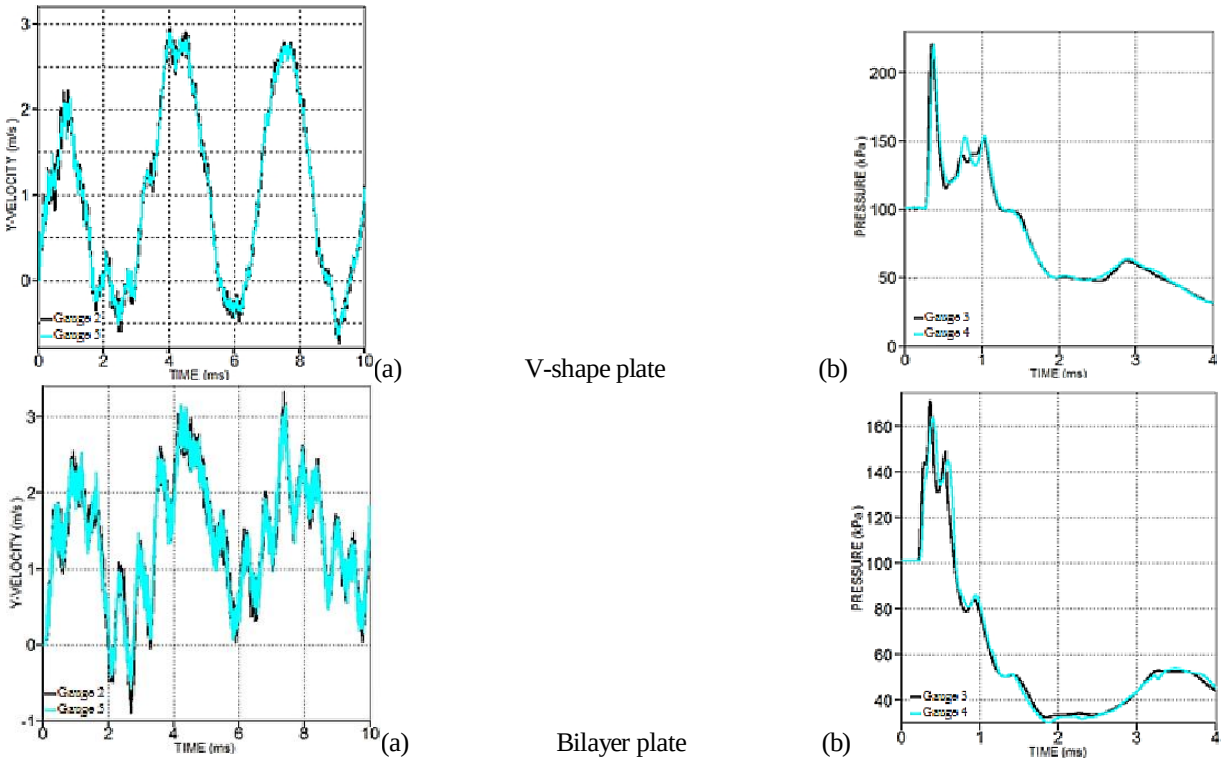

Fig. 9. The evolution of the parameters recorded by virtual sensors: (a) velocity, (b) overpressure

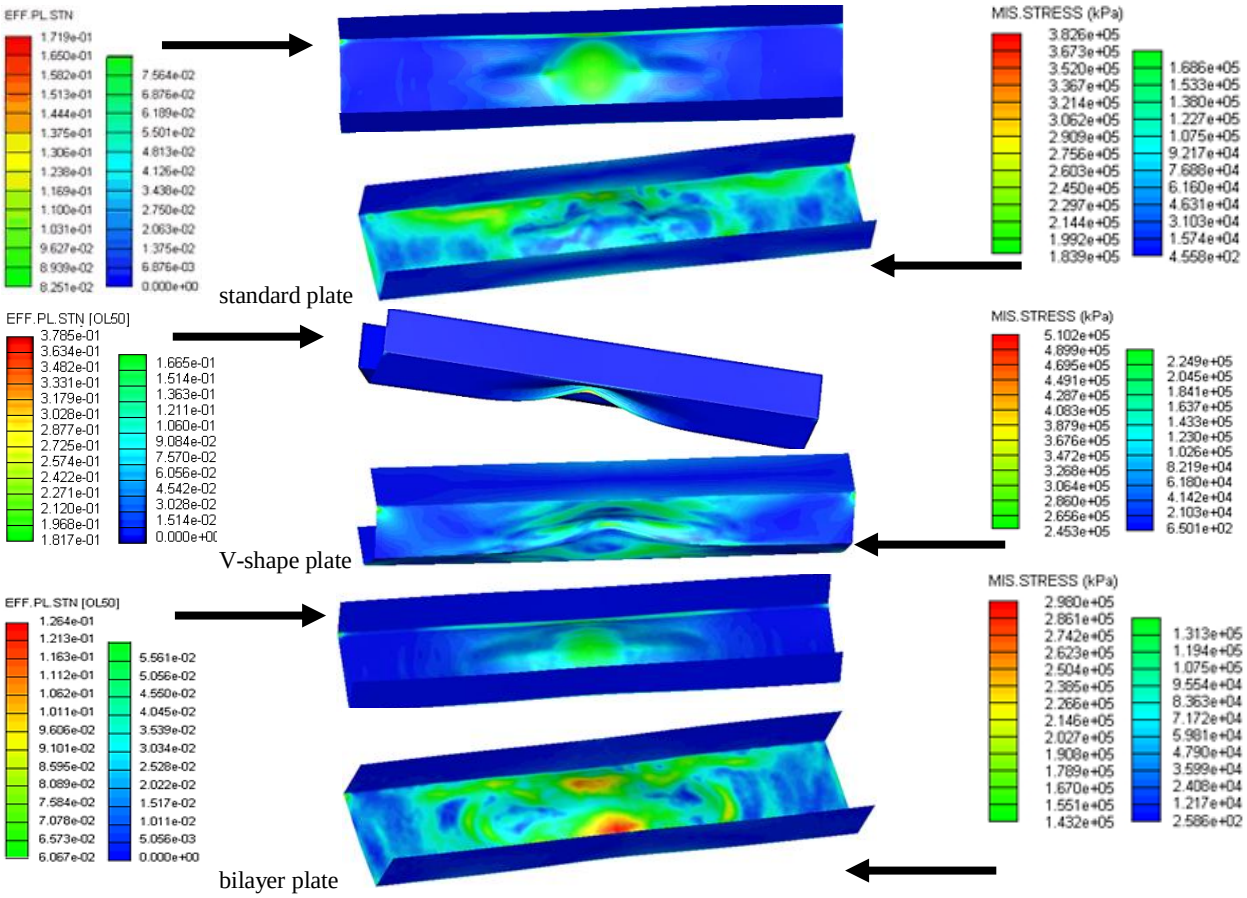

Fig. 10. Effective plastic strain Iso-values field at t=40 ms

4. RESULTS AND DISCUSSIONS

The experimental and numerical results allow a comparative analysis.
The findings for the two approaches compared against each other are detailed in Table 3.
In the case of experimental tests, for the calculation of the impulse transferred to the structure, the captured images were analyzed.

Table 3. Analysis of tested solutions

		Set1(standard plate)			Set 2(V-shape plate)			Set 3(bilayer plate)	
Experimental Test	Impulse (kg·m/s)	78.886	78.097	79.675	53.663	53.717	55.81	61.553	63.399
	Velocity (m/s)	1.712	1.695	1.729	1.153	1.154	1.191	1.322	1.362
	Transversal displacement(mm)	38.200	38.660	39.250	-	-	-	34.05	34.46
Numerical Simulation	Impulse (kg·m/s)	79.7			54.24			62.21	
	Velocity (m/s)	1.736			1.169			1.341	
	Transversal displacement (mm)	37.43			-			34.91	
Attenuation (%)		**0**			**32**			**22**	

Regarding the blast wave parameters, velocity and overpressure, the data recorded by real and virtual transducers were analyzed by using MathCAD software.

The structure velocity evolution induced by blast wave was determined by integrating the acceleration data as illustrated in Figure 11.

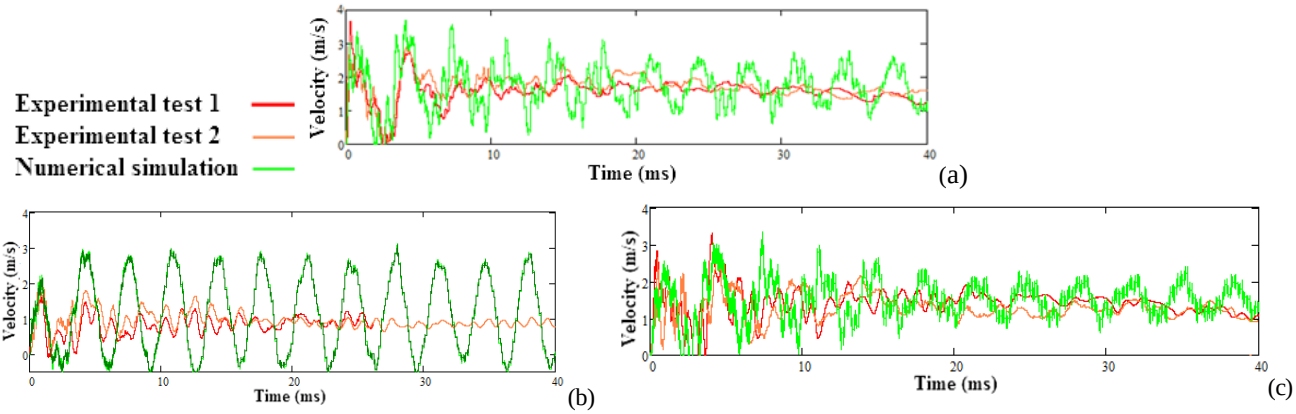

Fig. 11. Comparative analysis of the evolution of the velocity parameter: (a) standard plate, (b) V-shaped plate, (c) OL50-perlite plate

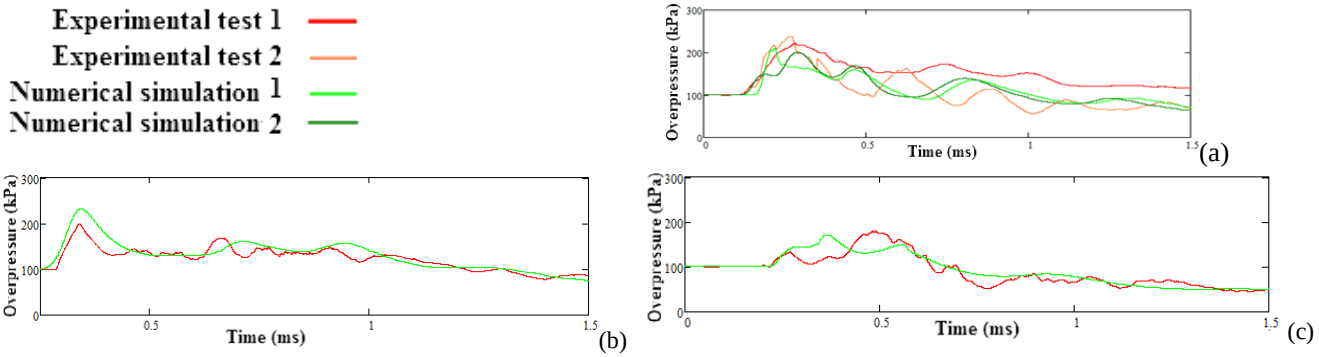

Fig. 12. Comparative analysis of the evolution of the overpressure parameter: (a) standard plate, (b) V-shaped plate, (c) OL50-perlite plate

Because after t = 1.5 ms the signals related with the pressure are altered by system inertia, the pressure data are presented only for 1.5 ms in Figure 12.

Unfortunately, the simplified hypotheses considered into the numerical model induce some discrepancy between the real and the virtual signals.

No vibrations damping options were used in the simulation.
The correspondence between numerical and experimental results has confirmed the validity of the proposed approaches.

5. CONCLUSIONS

An experimental and numerical study of shock wave/structure interaction has been performed for two impulse mitigation concept designs.
Using a V-shape and a bilayer plate configuration, the blast wave effects were studied for the same weight added to standard structure, approximatively 4000 g.
The values of the center plate deflection, the overpressure, respectively the velocity of the structure indicated a fair similarity between experimental and numerical data. The test results indicate that a V- shaped plate has a better behavior than the other two solutions (flat plate respectively bilayer plate), resulting in a 32% attenuation of the transferred impulse. The use of a perlite granular material indicated up to 22% impulse mitigation. This result can be encouraging with regard to the possibility of using this material along with other constructive solution, even V-shape plate in order to increase the protection level. The concept for the bilayer plate (OL50-perlite) allows, by using simple and easy-to-use technology, to improve the level of protection of military vehicles at minimal cost. Configurations can be set-up during missions, without the need to transport vehicles to a production facility.

6. REFERENCES

1. Baker, W. E., Cox, P.A., Westine, P.S., Kulesz, J.J., Strehlow, R.A., (1983).*Explosion hazards and evaluation*, (Amsterdam: Elsevier).
2.NATO AEP-55 STANAG 4965 "Protection Levels for occupants of Logistic and Light Armored Vehicles".
3. Zakrisson, B., (2010).*Numerical and Experimental Studies of Blast Loading*, Licentiate Thesis, Printed by Universitetstryckeriet, Luleå University of Technology, Örnsköldsvik.
4. Chung, S., Nurick, G.N., (2005).*Experimental and numerical studies on the response of quadrangular stifened plates. Part I: subjected to uniform blast load*, Int. J. of Impact Engineering, **31**,55-83.
5. Bucur, F., (2015). *Contributions to improve protection factor of military vehicles armor* - PhD thesis, Military Technical Academy, Bucharest.
6. Fink, B.K., (2000). *Performance Metrics for Composite Integral Armor*, ARL-RP-8, Aberdeen Proving Ground, Md.: Army Research Laboratory.
7. Rotariu, A., Bucur, F., Toader, G., Lupoae, M., Sava, A.C., Somoiag, P., Cirmaci-Matei, M. V., (2016). *Experimental Study on Polyurea Coating Effects on Deformation of Metallic Plates Subjected to Air Blast Loads*, Mat. Plast., **53**(4), 670-674.
8. Turtoi, P., Pascovici, M. D., Cicone, T., Rotariu, A., Puică, C., Istrate, M., (2019). *Optimal porosity for impact squeeze of soft layers imbibed with liquids*, Tribology International, **138**, 140-149.
9. Nedelcu D., Milosevic O., Chelariu R., Roman C, (2010). *Some experimental aspects concerning the stratified composite materials with metallic matrix*, Int. J. of Modern Manuf. Technologies, **II (2)**, 65-71.
10. Nedelcu D., Carcea I., (2013). *Technology for obtaining samples of layered composite materials with metallic matrix*, Metals and Materials International **19**(1), 105-112.
11. Fradinho J., Nedelcu D., Gabriel-Santos A., Gonçalves-Coelho A., Mourão A., (2015). *Some trends and proposals for the inclusion of sustainability in the design of manufacturing process*,IOP conf series:Materials science and engineering **95**(1), 012142
12. Sava A.C., Cherecheş T., Vedinaş I., Ionescu C., Piticari L., (2010). *Particularities regarding the Launching System of Ahead Projectiles*, Proceedings of the 16th International Conference–The Knowledge-Based Organization, 501-504.
13. Sava A.C., Bârsan Gh., Vedinaș I., Piticari L., (2016). *The impact of kinetic projectiles of 76 mm cal. ahead type artillery ammunition on the lifting surface of the aerospace vehicles*, Review of the Land Force Academy **21**(1), 92-98.
14. http://www.army-technology.com;Accesed on: 14.02.2019
15. http://www.military-today.com;Accesed on: 15.02.2019
16. Kumar, P., Leblanc, J., Stargel, D. S., Shukla, A., (2012). *Effect of plate curvature on blast response of aluminum panels*, Int. J. of Impact Engineering, **46**, 74-85.
17. Chung Kim Yuen,S.,Langdon,G.S.,Nurick,G.N., Pickering,E.G., Balden, V.H.,(2012). *Response of V-shape plates to localized blast load: Experiments and numerical simulation*, Int J. of Impact Engineering, **46**, 97-109.
18. Fišerová,D., (2006). *Numerical analyses of buried mine explosions with emphasis on effect of soil properties on loading*, PhD thesis, Cranfield University.
19. Matache, L., Puica, C., Rotariu, A., Tranã, E., Bucur, F., (2018). *Numerical simulation of military ground vehicle's response to mine-blast load*, Scientific Bulletin, Series D: Mechanical Engineering, **80**(4), 153-162.
20. Hargather, M. J., Settles, G. S., (2009).

Laboratory-scale techniques for the measurement of a material response to an explosive blast, Int. J. of Impact Engineering, **36**, 940-947.
21. Gupta, K. K., Meek, J. L., (1996). *A brief history of the beginning of the finite element method*, Int. J. for Numerical Methods in Engineering, **39**, 3761-3774.
22. Nicola I., Todirica C., Plesa C., Predoi C., Sava A.C., (2019). *Thermomechanical Analysis of Ertalon 4.6 Polyamide Used in High Thermal Shock Systems*, Mat. Plast., **56**(4), 942-947.
23. Wang, B., Zhang, J., LU, G., (2001). *Taylor impact test for ductile porous materials-Part 1: Theory*, Int. J. of Impact Engineering, **25**, 981-991.
24. Rotariu, A., Trană, E., Dima, C., Enache C., Timplaru, F., Matache, L., (2016).*Uninstrumented measurement method for granular porfous media blast mitigation assessment*, Experimental Techniques, **40**(3), 993-1003.
25. Bucur, F., Rotariu, A., Trana, E., Matache, L., (2016). *Experimental study regarding transferred impulse mitigation by perlite layer,* Int. J. of Mechanical and Production Engineering, **4**(8), 27-30.

Received: April 30, 2020 / Accepted: June 15, 2020 / Paper available online: June 20, 2020